Electron attachment to CF3 and CF3Br at temperatures up to 890 K: Experimental test of the kinetic modeling approach

Nicholas S. Shuman, Thomas M. Miller, Albert A. Viggiano, and Jürgen Troe

Citation: J. Chem. Phys. **138**, 204316 (2013); doi: 10.1063/1.4807606
View online: http://dx.doi.org/10.1063/1.4807606
View Table of Contents: http://jcp.aip.org/resource/1/JCPSA6/v138/i20
Published by the AIP Publishing LLC.

Electron attachment to CF_3 and CF_3Br at temperatures up to 890 K: Experimental test of the kinetic modeling approach

Nicholas S. Shuman,[1] Thomas M. Miller,[1] Albert A. Viggiano,[1,a)] and Jürgen Troe[2,3]
[1]*Air Force Research Laboratory, Space Vehicles Directorate, Kirtland Air Force Base, New Mexico 87117, USA*
[2]*Institut fur Physikalische Chemie, Universität Göttingen, Göttingen, Germany*
[3]*Max-Planck-Institut für Biophysikalische Chemie, Tammannstrasse 6, D-37077 Göttingen, Germany*

(Received 22 March 2013; accepted 8 May 2013; published online 31 May 2013)

Thermal rate constants and product branching fractions for electron attachment to CF_3Br and the CF_3 radical have been measured over the temperature range 300–890 K, the upper limit being restricted by thermal decomposition of CF_3Br. Both measurements were made in Flowing Afterglow Langmuir Probe apparatuses; the CF_3Br measurement was made using standard techniques, and the CF_3 measurement using the Variable Electron and Neutral Density Attachment Mass Spectrometry technique. Attachment to CF_3Br proceeds exclusively by the dissociative channel yielding Br^-, with a rate constant increasing from 1.1×10^{-8} cm^3 s^{-1} at 300 K to 5.3×10^{-8} cm^3 s^{-1} at 890 K, somewhat lower than previous data at temperatures up to 777 K. CF_3 attachment proceeds through competition between associative attachment yielding CF_3^- and dissociative attachment yielding F^-. Prior data up to 600 K showed the rate constant monotonically increasing, with the partial rate constant of the dissociative channel following Arrhenius behavior; however, extrapolation of the data using a recently proposed kinetic modeling approach predicted the rate constant to turn over at higher temperatures, despite being only ∼5% of the collision rate. The current data agree well with the previous kinetic modeling extrapolation, providing a demonstration of the predictive capabilities of the approach. [http://dx.doi.org/10.1063/1.4807606]

INTRODUCTION

Electron attachment processes have garnered experimental and theoretical attention for decades;[1–3] however, the sensitivity of the phenomenon to the specifics of the potential surface has limited the efficacy of predictive models of its kinetics. Even a broad statement of whether a particular system at a particular energy will attach to yield a stable anion either rapidly, slowly, or not at all is exceptionally difficult to answer absent experimental results, regardless of whether information on the system such as the electron affinity is well-established.[4,5]

In principle, high-level theoretical approaches, such as R-matrix theory,[5–9] can account for the interaction between the incident electron and nuclear motions of the neutral molecule, and yield kinetic data such as cross-sections and product branching. In practice, such methods are arduous and only applicable to small systems comprising a handful of atoms. Additionally, results from some systems on which such calculations have been performed were later found to be at odds with experimental results.[6,9–11]

Over the past several years an alternative approach of applying kinetic modeling to an attaching system has been developed,[12–14] with continued success in replicating experimental results.[11,15,16] As opposed to first-principles approaches, kinetic modeling involves only simple calculation and requires only modest information of the potential energy surface. The approach is to reduce the attachment process as far as possible into discrete steps, and then treat each individually through either statistical theory or, for the most complicated steps such as coupling of the electron and nuclear motions, through functional forms with empirically validated adjustable parameters. While reproducing experimental results is encouraging, and provides some insight into the dynamics of the processes, the major utility of kinetic modeling lies in the ability to extrapolate results to conditions inconvenient or inaccessible to experiment. Here we present a demonstration of such an extrapolation.

Coincident with the development of the kinetic modeling approach to electron attachment, we have developed a novel experimental technique using a Flowing Afterglow Langmuir Probe (FALP) apparatus.[17] The technique, dubbed Variable Electron and Neutral Density Attachment Mass Spectrometry (VENDAMS), allows for study of electron attachment to unstable species such as radicals,[11,18–20] rate constants and neutral product branching fractions of mutual neutralization reactions,[21,22] rate constants of dissociative recombination, and has provided evidence that a high density of electrons enhances the rate of mutual neutralization.[23,24]

Because no method prior to VENDAMS was sufficiently general to allow measurement of the kinetics of thermal electron attachment to a wide range of radicals, the literature data were limited, consisting of just two values.[25] In particular, no data on thermal electron attachment to fluorocarbon radicals existed; these data are particularly important because they are needed for predictive modeling of plasma etching of semiconductor material, a vital industrial process involved in the fabrication of microelectronics. We have previously reported rate constants and product branching for most small

a)Author to whom correspondence should be addressed. Electronic mail: afrl.rvborgmailbox@kirtland.af.mil

fluorocarbon radicals (CF_2, CF_3, C_2F_3, C_2F_5, 1-C_3F_7, 2-C_3F_7, 3-C_3F_5) from 300 to 600 K.[11,18,19] In concert, a separate beam experiment provided relative cross sections of attachment to CF_2[10] and C_2F_5[18] as a function of electron energy up to 10 eV. Kinetic modeling was used to extrapolate these data to conditions most relevant to plasma etching, namely gas temperatures around 300 K and electron temperatures up to 10 000 K.

The CF_3 system is particularly intriguing because, due to a mild endothermicity for dissociative attachment, electron attachment (1) proceeds via a competition between associative attachment (2a), dissociative attachment yielding F^- (2b), and autodetachment (2c),

$$CF_3 + e \rightarrow CF_3^{-*}, \tag{1}$$

$$CF_3^{-*} + M \rightarrow CF_3^-, \tag{2a}$$

$$CF_3^{-*} \rightarrow CF_2 + F^-, \tag{2b}$$

$$CF_3^{-*} \rightarrow CF_3 + e. \tag{2c}$$

This is a richer system than the other fluorocarbon radicals, which either do not attach to form a stable anion at thermal energies (namely, CF_2), or have unity branching to dissociative attachment to yield F^-. Both pressure and temperature dependences of the overall rate constant for attachment to CF_3 (the former being the first such dependence reported in the pressure range of ~1 Torr) and of the partial rate constants of the product channels were measured. Kinetic modeling reproduced all of these data, with an interesting implication as described in the following.

The rate constant of the dissociative channel (2b) over the measured range of 300–600 K increases rapidly and may be described by an Arrhenius equation with an activation energy of 0.21 eV. This behavior is commonly seen in inefficient electron attaching systems,[5,26] such as CF_3, which attaches at just 2% of the collision rate at 300 K. Typically, the attachment rate constant will turn over with increasing temperature as it approaches the collision rate. In this case, application of the kinetic modeling predicted the CF_3 rate constant to deviate from Arrhenius behavior at temperatures just above the measured range, despite the efficiency of the attachment remaining below 4% of the collision rate. Here, we have extended the VENDAMS measurements of attachment to CF_3 up to 890 K using a FALP apparatus designed for high temperature experiments[27] (HT-FALP) in order to test the previous extrapolation made using the kinetic modeling.

In order to perform these experiments, it is necessary to measure the kinetics of attachment to a neutral precursor for CF_3, in this case CF_3Br. CF_3Br happens to be one of the most studied systems for electron attachment, with measurements of thermal rate constants by several groups and techniques up to as high as 777 K.[28–31] Additionally, owing to the wealth of experimental data, the system was used as a standard to empirically evaluate the functional forms used in the kinetic modeling to separate contributions from the electronic and nuclear motions.[14] Here we also report electron attachment rate constants for CF_3Br, extending those measurements up to 890 K using traditional FALP techniques for this stable molecule, as opposed to the VENDAMS method used to measure attachment to radicals.

EXPERIMENTAL

The primary experimental distinction between the current study and our prior lower temperature study involves the nature of the apparatus. While both use implementations of the classic FALP setup, the experiments here were performed using a machine (HT-FALP) designed to tolerate temperatures up to 1400 K using, as here, a quartz flow tube, or 1800 K using a ceramic one. This apparatus,[27] the traditional technique of measuring electron attachment using a FALP,[32] and the VENDAMS method[17] all have been described in detail elsewhere; the most relevant aspects will be repeated here.

A helium (99.999% Matheson) flow of between 10 and 25 std. L min^{-1} enters a 1 m long, 7 cm diameter quartz flow tube. Upstream of the flow tube, the helium is discharged in an Evenson microwave cavity producing an afterglow plasma consisting of He^+, He_2^+, He^*, and e. An argon flow of 0.5–3 std. L min^{-1} is added downstream of the discharge, converting He_2^+ and He^* to Ar^+. The positive charge of the resulting electron/ion plasma is between 50% and 95% Ar^+, depending on the gas density and the efficiency of the $He^+ + He \rightarrow He_2^+$ reaction prior to introduction of Ar, with the remainder primarily He^+ with trace other species arising from water and air contaminants. The gas pressure in the flow tube is maintained between 1 and 2 Torr by a throttled Roots pump located at the downstream end. Reactant gas may be added through a quartz inlet consisting of 4 radial, hollow needles and located 53 cm from the ion sampling orifice at the end of the flow tube.

The apparatus contains two diagnostics: a mass spectrometer and a Langmuir probe. The center of the flow is sampled downstream through a pinhole aperture into a high vacuum region containing an electrostatic lens assembly and a quadrupole ion mass filter. Relative ion abundances are monitored using an electron multiplier operating in counting mode. The Langmuir probe, a 76 μm diameter, 7.6 mm long tungsten wire, is moveable from 1 to 30 cm downstream of the reactant inlet, providing absolute measurements of the electron concentration along the center axis. The electron density is variable from ~10^8 cm^{-3} (the minimum practical reading of the Langmuir probe) to up to 10^{10} cm^{-3} depending on the particular temperature and pressure conditions. The plasma density is varied primarily by varying the fraction of the helium flowing either through the discharge or through a separate inlet downstream of the discharge, and varied to a lesser extent by the distance between the microwave cavity and the flow tube and by the microwave power.

The entirety of the flow tube is surrounded by a commercial oven, which is in turn surrounded by an exterior vacuum box maintained at ~10^{-3} Torr by a Roots pump. In order to maintain a constant temperature profile throughout the reaction length, gas passing through the upstream end of the flow tube must be preheated 10%–20% above the desired temperature. The reactant gas inlet line passes through this overheated zone of the flow tube, limiting the maximum temperature to that at which the preheating causes thermal decomposition of

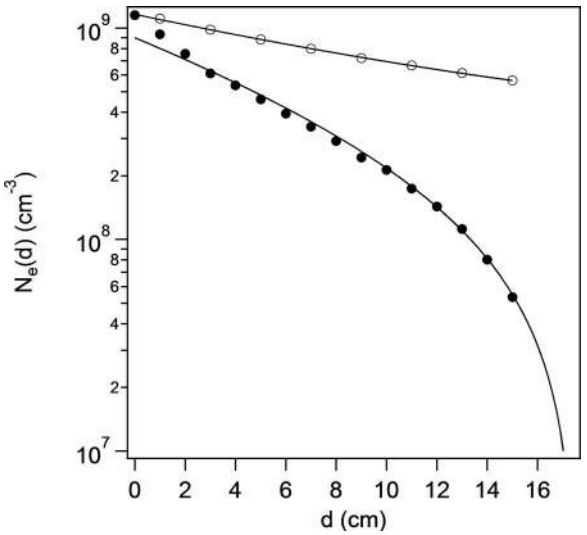

FIG. 1. Sample data measuring electron attachment to CF_3Br at 800 K, showing the electron density decay due to diffusive loss (open circles) and due to the combination of diffusive loss and addition of 2.7×10^{10} cm^{-3} CF_3Br (solid circles). The lines through the data are solutions to the relevant rate equations. The first 3 cm are slightly disturbed by the reactant inlet.

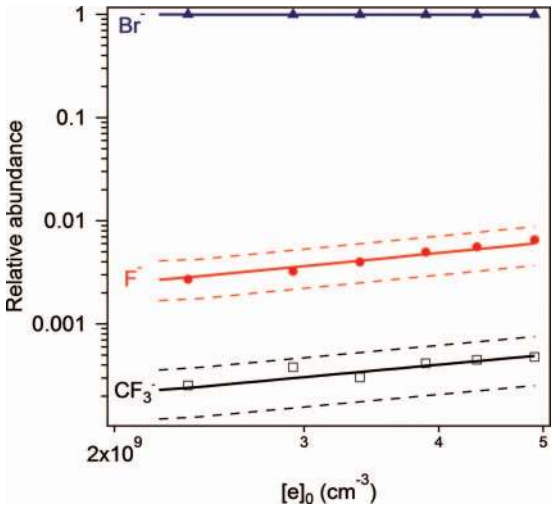

FIG. 2. An example of VENDAMS data measuring electron attachment to CF_3 showing relative product anion abundances 1.9 ms after addition of 1.4×10^{10} cm^{-3} CF_3Br to the flowing afterglow at 700 K and 1 Torr. Points are measured abundances, solid lines are best fit calculated abundances (see text), and dashed lines are example fits at the edges of the uncertainty limits.

the reactant molecules (presumably by reaction on the hot walls). In the case here of CF_3Br, thermal decomposition in the inlet line occurs near 1000 K, limiting experiments to $T < 900$ K.

In the traditional FALP method, a reactant gas (e.g., CF_3Br) is added through the reactant inlet at sufficient concentration to significantly deplete the electron density within 10–20 cm (typically $\sim 10^{12}$ cm^{-3}). The reactant flow is controlled by a 10 std. cm^3 min^{-1} mass flowmeter (MKS). The electron density is measured as a function of distance by translating the Langmuir probe along the flow tube. Distance is equated to time by the measured plasma velocity, determined either directly by pulsing the microwave discharge and noting the arrival time of the pulse as a function of distance using the Langmuir probe, or taken as 1.7 times the buffer velocity as calculated from the known flow rates, temperature, and pressure. The attachment rate constant is derived by the loss rate of electrons, taking into account the ambipolar diffusion rate, as measured by monitoring the disappearance of electrons along the flow tube with no reactant gas added. An example of the data is shown in Figure 1.

In the VENDAMS method to measure radical electron attachment, the same reactant gas is added in a much lower concentration ($\sim 10^{10}$ cm^{-3}) and the Langmuir probe is held stationary, monitoring the electron density at the reactant inlet, $[e]_0$. The primary data in VENDAMS are the relative anion concentrations measured using the quadrupole mass spectrometer at the end of the flow tube after a fixed reaction time as a function of $[e]_0$ (Figure 2). Primary attachment to CF_3Br (3) yields exclusively CF_3 and Br^-,

$$CF_3Br + e \rightarrow CF_3 + Br^-. \quad (3)$$

At low plasma densities reaction (3) will quickly deplete the electron concentration and further processes occur to only a minor extent. As the plasma density increases, concentrations of both the product CF_3 and remnant electrons increase resulting in an increasingly significant amount of attachment to CF_3 (1). The extents of associative (2a) and dissociative (2b) attachment to CF_3 are reflected by the magnitudes of the abundances of CF_3^- and F^- relative to Br^-. Because they are products of secondary attachment (i.e., as opposed to Br^- being a product of the primary attachment) the abundances of F^- and CF_3^- increase directly with $[e]_0$ with a proportionality constant of about 1. CF_3^-, being a polyatomic species, undergoes mutual neutralization with the atomic cations that dominate the afterglow, while F^- and Br^- do not to any significant extent at these densities.[22,33] As a result, the CF_3^- abundance shows additional curvature at higher densities, although this is not apparent in Figure 2 (see, for instance Figure 1 of Ref. 11). The rate constants of each process are derived by iteratively solving the set of coupled differential describing the dominant reactions occurring in the afterglow from the known initial condition throughout the reaction time, and comparing the resulting calculated abundances to those measured; the full process is described in Refs. 17 and 24.

Any error in accounting for detection discrimination between F^-, Br^-, and CF_3^- propagates linearly into the derived rate constants. Discrimination for this instrument has been found to be a function of both mass and whether the ion is atomic or molecular. Discrimination between Br^- and F^- was measured by flowing first CH_3Br, which attaches electrons to yield Br^-, measuring the depletion of the electron density 10 cm downstream of the reactant inlet and noting the height of the Br^- peak on the mass spectrometer. Under the same conditions NF_3, which attaches electrons to yield F^-, was flowed in a concentration to cause the same depletion in the electron density. The ratio of the F^- to the Br^- peak heights is the discrimination ratio. A series of measurements gave an average value of 2 favoring detection of F^-; however, the measurement could not be performed close in time to the VENDAMS experiments, because remnant NF_3 in the reactant line resulted in a large baseline F^- signal. As a

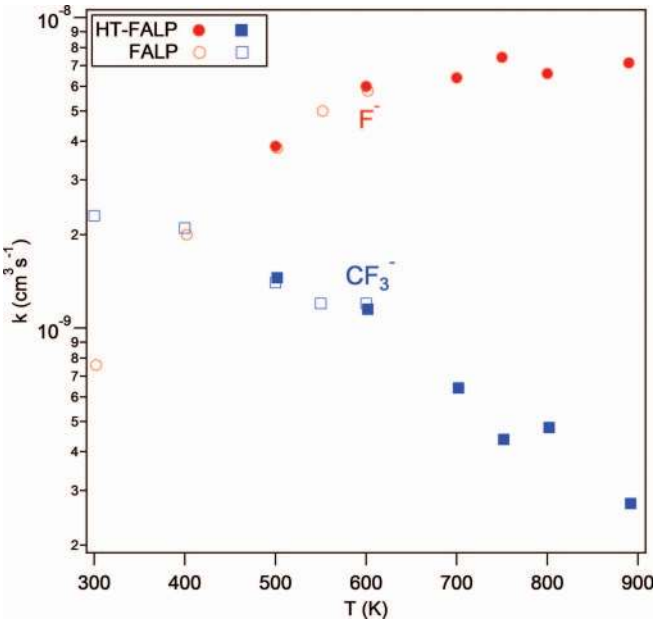

FIG. 3. Comparison of partial rate constants of electron attachment to CF_3 at a constant number density of 3.2×10^{16} cm^{-3} reported in the current study (HT-FALP) with previously reported values at lower temperature (FALP). Error bars are omitted from the plot for clarity, but are 30%–60% of the base value.

consistency check, VENDAMS measurements were made at 500 K and 600 K, overlapping with previously reported measurements (Figure 3). The current data agree with the literature data assuming a discrimination factor of 2.1, in good agreement with the above discrimination measurement.[11] We do not have means to measure the CF_3^- discrimination. In previous experiments using the standard temperature FALP,[11] the discrimination factor was deduced from a calibration curve of factors measured for a wide range of species as described in Ref. 34, but these same measurements are not possible with the high temperature FALP due to a lack of a second downstream reactant inlet. Instead, the CF_3^- discrimination factor was determined solely by comparison with the literature data for CF_3 attachment; the factor was found to be 1.2 relative to F^-.

RESULTS AND DISCUSSION

The thermal rate constants for electron attachment to CF_3Br were measured from 500 K to 890 K using the HT-FALP apparatus (Figure 4) and from 300 to 500 K using the standard FALP. The latter measurements fall slightly (~10%) below recently published values by our group using the same method and apparatus;[16] an average of the current and prior measurements is reported here. Attachment is exclusively dissociative yielding Br^-, and is increasingly efficient as the temperature approaches 1000 K, about the point at which CF_3Br thermally decomposes. Both sets of current data are smaller than literature values from three prior experiments at 300 K and above, which appeared to have a consensus.[28–30] Two attempts at calculating thermal rate constants for attachment to CF_3Br have been made, both using the data set that existed prior to our group's two recent studies. Both R-matrix

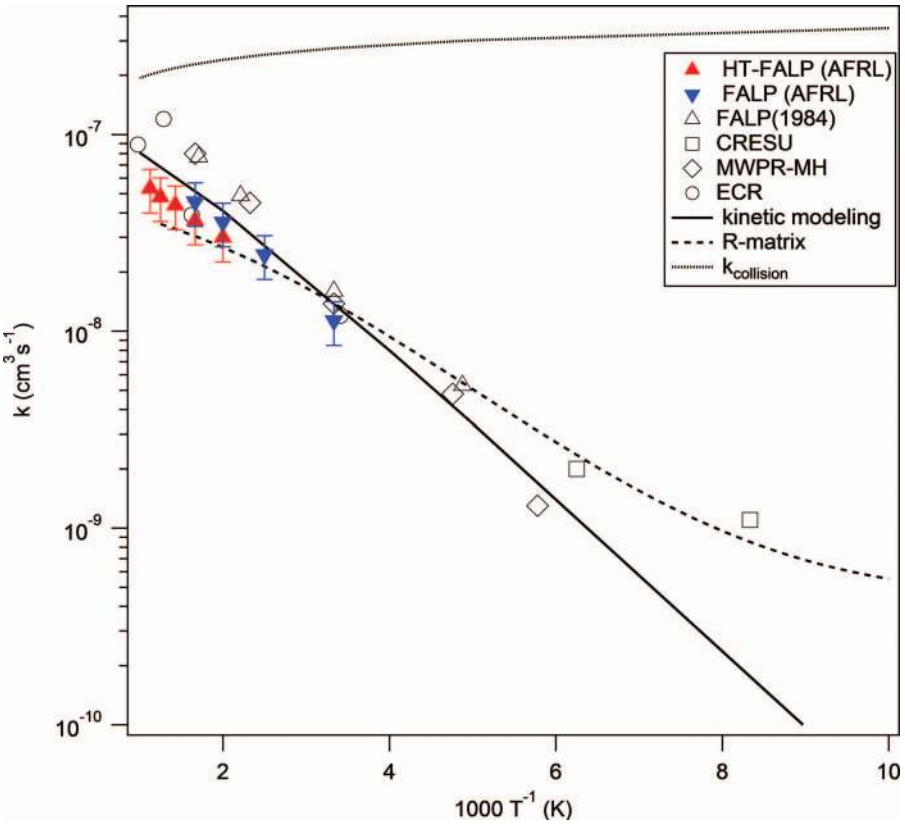

FIG. 4. Thermal rate constants for electron attachment to CF_3Br at the indicated temperatures. Solid triangles: this work; open triangles: Ref. 29; open squares: Ref. 37; open circles: Ref. 30; open diamonds and dashed line: Ref. 28; solid line: Ref. 14.

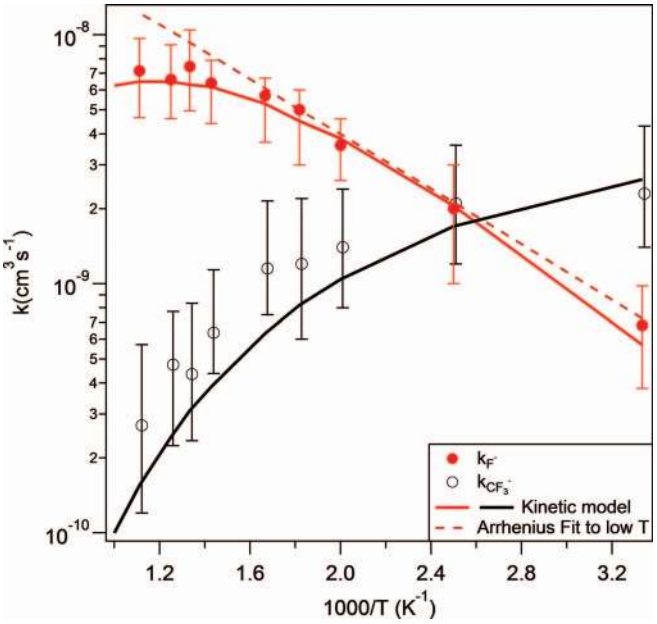

FIG. 5. Partial rate constants of electron attachment to CF_3 at a constant number density of 3.2×10^{16} cm^{-3} from current and prior studies. Solid lines are the best fit from kinetic modeling; the dashed line is a fit with the Arrhenius equation to the data from 300 to 600 K.

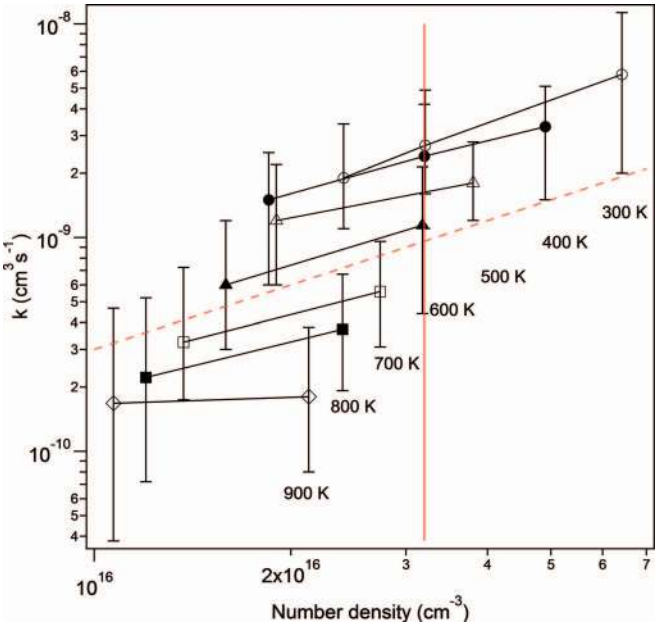

FIG. 6. Partial rate constants for associative attachment to CF_3 (i.e., $CF_3 + e \rightarrow CF_3^-$) at the indicated temperatures as a function of buffer gas number density. The dashed line is a linear relationship with slope of 1 to guide the eye; the vertical line indicates the number density for data reported in Figures 3 and 4.

calculations by Hotop, Fabrikant, and co-workers[5,28] and kinetic modeling by Troe *et al.*[14] fell significantly below the experimental rate constants above 400 K available at the time, while being in good agreement with data between 200 and 300 K. The current CF_3Br attachment rate constants are in better agreement with both calculations. There is some reason to believe that the prior experiments reported elevated rate constants at higher temperatures. Electron attachment rate constants reported using the Birmingham FALP[29] apparatus in the 1980s have generally been somewhat elevated compared to other measurements.[35] Additionally, the ECR measurements[30] were normalized to the electron attachment rate constant for SF_6, which was assumed to be temperature independent; however, it is now known to decrease at higher temperatures.[36]

Rate constants for thermal electron attachment to CF_3 were measured using the VENDAMS method from 500 K to 890 K. The partial rate constants for associative and dissociative attachment as a function of temperature at a constant number density appear in Figure 5. The data have been combined with literature values from 300 to 600 K.[11] Data were taken at pressures of 1 and 2 Torr at each temperature. Values reported in Figure 5 are either linearly interpolated or extrapolated as needed to a fixed number density of 3.2×10^{16} cm^{-3}. Partial rate constants for associative attachment at the measured number densities appear in Figure 6, justifying the linear extrapolations (partial rate constants for dissociative attachment are found to be independent of number density, and the reported values in Figure 5 are averages of all data taken at the indicated temperature).

A qualitative explanation for the temperature and pressure trends accompanied the previously published, lower temperature data. As the temperature increases, an increasingly larger fraction of the CF_3 thermal internal energy distribution exceeds the 0.22 ± 0.02 eV threshold to dissociative attachment. Because dissociation of CF_3^{-*} is fast relative to autodetachment or stabilization, the result is a steep rise in the partial rate constant for dissociative attachment and a decline in the partial rate constant for associative attachment. As the pressure increases for a fixed temperature, the number of collisions of CF_3^{-*} with the buffer gas increases. That the rate constant of associative attachment is seen to approximately scale with the number density with a slope of 1 indicates that the system is in the low pressure limit of reactivity.

More insight is gained by evaluating the system through kinetic modeling, details of which have been presented in Refs. 13, 14, and 17. Briefly, the attachment process is separated into discrete steps consisting of (1) the incident electron and neutral molecule create a "contact pair;" (2) depending on its lifetime, coupling between the electron and nuclear motions, and any energy barrier to the crossing between the neutral and anion surface, the "contact pair" may lead to an excited anion state (CF_3^{-*}); (3) the excited anion state will decay through a competition of electron autodetachment, dissociation to neutral and anion fragments, or stabilization to the parent anion either radiatively or through collision with a third-body (associative attachment). Step (1) is treated by calculating a collisional cross-section (σ_{cap}) as a function of electron energy using extended Vogt-Wannier theory, for which analytical forms for polarizable dipolar species have been developed.[38,39] Under the assumption that incorporating the incident electron into the electron cloud of the neutral takes a finite amount of time, the attachment cross-section (σ_{at}) is calculated by reducing the capture probability from the Vogt-Wannier value as a function of electron energy using the functional form

$$\sigma_{at} = \sigma_{cap} P_{IVR}(T_{el}) P_{nuc}(T_{gas}), \quad (4)$$

$$P_{IVR} = e^{-c_1\kappa}, \tag{4a}$$

$$P_{nuc} = e^{-\left(\frac{E_{n,0}}{kT_{gas}}\right)}, \tag{4b}$$

where κ is proportional to the isotropic polarizability of the neutral and the square root of the electron energy, and c_1 is an empirically fit parameter. Where data exist, (4) may be refined by accounting for cusps in the capture probability resonant with vibrational modes of the neutral as a result of competition with electron scattering; however, only the simpler form is employed here. The capture probability is further reduced by the presence of any energetic barrier to cross to the anion surface. This is accounted for here using a simple step function convoluted over a direct count of the energy in internal modes of the neutral,[13] with the capture probability set to zero for any distribution with less than a value $E_{n,0}$, which is treated as an adjustable parameter, in a designated critical mode or modes. It is important to note that the crossing between the neutral and anion surface may be of multimodal character and does not necessarily correspond to critical mode(s) involved in dissociation of the anion. Calculation of the height of any barrier then involves the calculation of the full potential surfaces of both the neutral and anion and is not attempted here. CF_3^{-*} must be stabilized by one of the three aforementioned processes. Both autodetachment and dissociation are treated by calculating specific rate curves using unimolecular statistical theory. The autodetachment rate curve is a function of P_{IVR} through microscopic reversibility. The dissociation rate curve is calculated using the Simplified Statistical Adiabatic Channel Model,[40–42] which employs Orbiting Transition State-Phase Space Theory as a starting point. Finally competition between autodetachment, dissociation, and stabilization through collision with the buffer gas (radiative stabilization is too slow to compete here) is calculated by approximating the solution to the Master Equation using the Many-Shots approach.[11,43]

By inspection of Figure 5, the kinetic modeling reproduces the associative and dissociative attachment rate constants quite well. Although not shown, the kinetic modeling also reproduces the pressure dependences of the partial rate constants. The fits shown are the best fits to the full data set, but differ only slightly from the previously reported fits to the lower temperature data. The observed dissociative attachment rate constant begins to deviate from Arrhenius behavior as early as 600 K, in agreement with the previously reported extrapolations from the lower temperature data. Based on subsequent work, the form of P_{IVR} utilized in the lower temperature study, wherein κ is proportional to the electron energy was found to be slightly less desirable than having κ proportional to the square root of the electron energy, as employed here.

The rate constants of attachment for other systems have been observed to bend over at higher temperatures as they approach the collision rate. However, the collision rate constant for attachment to CF_3, as calculated using extended Vogt-Wannier theory, is 1.8×10^{-7} cm^3 s^{-1} at 900 K; that is, the measured attachment rate constant is less than 4% of the collision rate. Instead, as interpreted through the kinetic modeling, the limitation on the CF_3 attachment is due to the interplay of the electronic and nuclear motions. At low temperatures, attachment is hindered by the energetic barriers to cross from the neutral to the anion surface and to dissociation of CF_3^-; CF_3 with low internal energy cannot attach to form either product. In the region where this factor dominates, the rate constant of the dissociative attachment channel follows Arrhenius equation behavior. At higher temperatures, attachment is hindered by the difficulty of incorporating higher energy electrons into the neutral molecule prior to the separation of the contact pair. Essentially, there is a positive relationship between T_{gas} and k_{attach}, and a negative relationship between T_{el} and k_{attach}. In these thermal experiments where $T_{gas} = T_{el}$, the counteracting factors will result in a peak in the electron attachment rate constant. The CF_3 attachment rate constant is observed to turn over as it approaches that peak, and would be expected to decrease at still higher temperatures (CF_3 should be thermally stable to much higher temperatures than is CF_3Br).

At the conditions of the experiments here, electrons are rapidly thermalized[44] and none exceed about 0.5 eV. As a result, all attachment is assumed to arise from the so-called "zero-energy" peak; in the case of CF_3 arising from crossing from the ground electronic state of the neutral to the ground electronic state of the anion. Should higher energy resonances exist, e.g., involving electronically excited anion surfaces, the cross-section of attachment may show higher energy peaks, and experimental results would deviate from the extrapolation from our thermal data. R-matrix calculations suggest that no higher energy resonances exist for CF_3,[6] and the only experimental data on similar systems (CF_2[10] and C_2F_5[18]) show no higher energy resonances up to 10 eV. It appears reasonable that extrapolation of the current CF_3 data up to T_{el} approaching 1 eV (several thousand K, the conditions most relevant to plasma etching) is appropriate; such extrapolations may be made from Figures 9–11 previously reported in Ref. 11.

CONCLUSION

Thermal rate constants for electron attachment to CF_3Br and CF_3 have been measured up to 890 K. CF_3Br attaches dissociatively to yield Br^-. The current rate constants are somewhat smaller than previous literature values, but are in better agreement with theoretical treatments of the system. Electron attachment to CF_3 is inefficient, never exceeding 4% of the calculated collision rate, and proceeds both associatively to yield CF_3^- and dissociatively to yield F^-. The partial rate constants show marked temperature and pressure dependences, with the dissociative channel increasingly dominating at higher temperatures. An extrapolation of prior data on attachment to CF_3 below 600 K using a kinetic modeling approach had predicted that the attachment rate constant, which was observed to monotonically increase up to 600 K, to begin to turn over at only slightly higher temperatures, despite the inefficiency of the process. The current data confirm the predicted behavior, providing a successful demonstration of the predictive capabilities of the method.

[1]L. G. Christophorou, D. L. McCorkle, and A. A. Christodoulides, *Electron-Molecule Interactions and Their Applications* (Academic, New York, 1984).
[2]D. Smith and P. Spanel, in *Linking the Gaseous and Condensed Phases of Matter: The Behavior of Slow Electrons*, edited by L. G. Christophorou, E. Illenberger, and W. F. Schmidt (Plenum Press Div Plenum Publishing Corp, New York, 1994), Vol. 326, pp. 487–493.
[3]M. A. Biondi, Phys. Rev. **84**, 1072–1072 (1951).
[4]E. Illenberger and B. M. Smirnov, High Temp. **38**, 829–833 (2000).
[5]I. I. Fabrikant and H. Hotop, J. Chem. Phys. **128**, 124308 (2008).
[6]I. Rozum, N. J. Mason, and J. Tennyson, New J. Phys. **5**, 155 (2003).
[7]J. Tennyson, J. D. Gorfinkiel, I. Rozum, C. S. Trevisan, and N. Vinci, Radiat. Phys. Chem. **68**, 65–72 (2003).
[8]I. Rozum, N. J. Mason, and J. Tennyson, J. Phys. B **36**, 2419–2432 (2003).
[9]I. Rozum, N. J. Mason, and J. Tennyson, J. Phys. B **35**, 1583–1591 (2002).
[10]K. Graupner, T. A. Field, and C. A. Mayhew, New J. Phys. **12**, 083035 (2010).
[11]N. S. Shuman, T. M. Miller, J. F. Friedman, A. A. Viggiano, A. I. Maergoiz, and J. Troe, J. Chem. Phys. **135**, 054306 (2011).
[12]J. Troe, T. M. Miller, and A. A. Viggiano, J. Chem. Phys. **127**, 244303 (2007).
[13]J. Troe, G. Marowsky, N. S. Shuman, T. M. Miller, and A. A. Viggiano, Z. Phys. Chem. **225**, 1405–1416 (2011).
[14]J. Troe, T. M. Miller, N. S. Shuman, and A. A. Viggiano, J. Chem. Phys. **137**, 024303 (2012).
[15]N. S. Shuman, T. M. Miller, A. A. Viggiano, and J. Troe, J. Chem. Phys. **134**, 094310 (2011).
[16]N. S. Shuman, J. F. Friedman, T. M. Miller, and A. A. Viggiano, J. Chem. Phys. **137**, 164306 (2012).
[17]N. S. Shuman, T. M. Miller, A. A. Viggiano, and J. Troe, in *Advances in Atomic, Molecular, and Optical Physics*, edited by E. Arimondo, P. R. Berman, and C. C. Lin (Elsevier, Oxford, 2012), Vol. 61, pp. 209–294.
[18]S. A. Haughey, T. A. Field, J. Langer, N. S. Shuman, T. M. Miller, J. F. Friedman, and A. A. Viggiano, J. Chem. Phys. **137**, 054310 (2012).
[19]N. S. Shuman, T. M. Miller, and A. A. Viggiano, J. Chem. Phys. **137**, 214318 (2012).
[20]N. S. Shuman, T. M. Miller, and A. A. Viggiano, J. Chem. Phys. **136**, 124307 (2012).
[21]N. S. Shuman, T. M. Miller, N. Hazari, E. D. Luzik, and A. A. Viggiano, J. Chem. Phys. **134**, 069901 (2011).
[22]T. M. Miller, N. S. Shuman, and A. A. Viggiano, J. Chem. Phys. **136**, 204306 (2012).
[23]N. S. Shuman, T. M. Miller, R. J. Bemish, and A. A. Viggiano, Phys. Rev. Lett. **106**, 018302 (2011).
[24]N. S. Shuman, T. M. Miller, J. F. Friedman, A. A. Viggiano, S. Maeda, and K. Morokuma, J. Chem. Phys. **135**, 024204 (2011).
[25]N. G. Adams, D. Smith, and C. R. Herd, Int. J. Mass Spectrom. Ion Process. **84**, 243–253 (1988).
[26]H. Hotop, M. W. Ruf, J. Kopyra, T. M. Miller, and I. I. Fabrikant, J. Chem. Phys. **134**, 064303 (2011).
[27]P. M. Hierl, J. F. Friedman, T. M. Miller, I. Dotan, M. MenendezBarreto, J. V. Seeley, J. S. Williamson, F. Dale, P. L. Mundis, R. A. Morris, J. F. Paulson, and A. A. Viggiano, Rev. Sci. Instrum. **67**, 2142–2148 (1996).
[28]S. Marienfeld, T. Sunagawa, I. I. Fabrikant, M. Braun, M. W. Ruf, and H. Hotop, J. Chem. Phys. **124**, 154316 (2006).
[29]E. Alge, N. G. Adams, and D. Smith, J. Phys. B: At., Mol. Opt. Phys. **17**, 3827–3833 (1984).
[30]R. G. Levy, S. J. Burns, and D. L. McFadden, Chem. Phys. Lett. **231**, 132–138 (1994).
[31]S. J. Burns, J. M. Matthews, and D. L. McFadden, J. Phys. Chem. **100**, 19436–19440 (1996).
[32]D. Smith, and P. Spanel, In *Advances in Atomic, Molecular, and Optical Physics*, edited by B. Bederson and A. Dalgarno (Elsevier Academic Press Inc, San Diego, 1994), Vol. 32, pp. 307–343.
[33]M. J. Church and D. Smith, J. Phys. D-Appl. Phys. **11**, 2199–2206 (1978).
[34]N. S. Shuman, T. M. Miller, C. M. Caples, and A. A. Viggiano, J. Phys. Chem. A **114**, 11100–11108 (2010).
[35]L. G. Christophorou, D. L. McCorkle, and A. A. Christodoulides, in *Electron-Molecule Interactions and Their Applications*, edited by L. G. Christophorou (Academic, New York, 1984), pp. 477–617.
[36]A. A. Viggiano, T. M. Miller, J. F. Friedman, and J. Troe, J. Chem. Phys. **127**, 244305 (2007).
[37]J. L. LeGarrec, O. Sidko, J. L. Queffelec, S. Hamon, J. B. A. Mitchell, and B. R. Rowe, J. Chem. Phys. **107**, 54–63 (1997).
[38]E. I. Dashevskaya, I. Litvin, E. E. Nikitin, and J. Troe, J. Phys. Chem. A **115**, 6825–6830 (2011).
[39]E. I. Dashevskaya, I. Litvin, E. E. Nikitin, and J. Troe, Phys. Chem. Chem. Phys. **10**, 1270–1276 (2008).
[40]J. Troe, Z. Phys. Chem. **223**, 347–357 (2009).
[41]W. Stevens, B. Sztaray, N. Shuman, T. Baer, and J. Troe, J. Phys. Chem. A **113**, 573–582 (2009).
[42]J. Troe and V. G. Ushakov, J. Phys. Chem. A **110**, 6732–6741 (2006).
[43]R. V. Serauskas and E. W. Schlag, J. Chem. Phys. **42**, 3009–3018 (1965).
[44]D. Trunec, P. Spanel, and D. Smith, Chem. Phys. Lett. **372**, 728–732 (2003).